Article

Lead Carboxylates and Chromatic Parameter Changes in Oil-Based Paintings Exposed to Volatile Organic Compounds

Izabela G. Silva, [a] *Benigno Sanchez* [b] *and Maria Cristina Canela* *,[a]

*aGrupo de Pesquisa em Química Ambiental (GPQA), Laboratório de Ciências Químicas,
Universidade Estadual do Norte Fluminense Darcy Ribeiro (UENF),
28013-602 Campos dos Goytacazes-RJ, Brazil*

*bAnalysis and Photocatalytic Treatment of Pollutants in Air Group (FOTOAir),
Centro de Investigaciones Energeticas, Medioambientales y Tecnologicas (CIEMAT),
Avenida Complutense, 40, 28040, Madrid, Spain*

Some of the main concerns when attempting to preserve artwork regard environmental factors, such as luminosity, temperature and, recently, even atmospheric pollution. From this perspective, volatile organic compounds (VOC) stand out due to the wide availability of contaminating sources in internal museum environments. Amongst artistic objects susceptible to VOC interference, paintings are more likely to undergo it because their stability is closely related to each component. Thus, it is crucial to comprehend the interaction between VOC and paintings, specifically those with inorganic and adhesive pigments, and evaluate changes in chromatic parameters and the formation of metallic carboxylates. Mock-ups of paintings were prepared with cadmium yellow, chromium oxide, ultramarine blue, linseed oil, and lead white or gypsum primer. Exposure was arranged within an airtight container containing a VOC-saturated atmosphere: formaldehyde, acetic acid, hexanal and 2-butanone oxime. Color alteration occurred for ultramarine blue (greenish coloration) and cadmium yellow (lost luminosity). Infrared analysis showed the formation of lead carboxylates (acetate, formate and hexanoate) in all pigments. Micrographs of ultramarine models, verified via scanning electron microscopy, showed that an otherwise flat and homogenous appearance replaced the granular aspect of the paint; the flat regions being indicative of carboxylate formation.

Keywords: carboxylates, pigment, degradation, color change, painting

Introduction

Artwork plays an essential role in the cultural heritage of people, much like their history, language, customs, and accumulated knowledge. Unfortunately, cultural heritage undergoes aging processes which affect its materials, many of which are caused by biological, chemical, and physical agents.[1] Conservation techniques have the great chore of preserving these materials as best as possible, thus raising awareness of the need for control over environmental conditions, such as light quantity, temperature, relative humidity and, as of recently, even atmospheric pollution.[2]

Atmospheric composition has greatly changed due to increased pollutant quantity and variety.[3,4] Internal air quality is of great significance within this context since concentrations of chemical and biological contaminants increase considerably in these environments due to poor/limited air circulation.[5] In addition to external pollutants, confined spaces have their own environmental emission sources, primarily those of volatile organic compounds (VOC).[6,7] Internal museum environments might be brought to attention because, within these spaces, there are several contaminating VOC sources caused by construction material, coatings, decor and finishes or materials used in manufacturing displays, such as paints and binders, as well as chemical products used to clean, restore and store.[8-11]

Acetic acid (CH_3COOH), formic acid ($HCOOH$) and formaldehyde (CH_2O) are often analyzed as VOCs due to their high corrosion potential.[2,3,12-14] Their emission sources are mainly objects, adhesive materials, paints and wooden furniture, artifacts which are quite common in museums.[15] Formaldehyde, significantly, has resin used in the manufacture of plywood, paper, plastic and

*e-mail: mccanela@uenf.br
Editor handled this article: Eduardo Carasek

fabrics as one of its main emission sources. Acetic acid may be released from acidic cure silicone employed when sealing displays. Other VOC currently found within these environments are siloxanes and oximes, released from neutral cure silicone used in modern displays[3,16,17] and aldehydes emitted by cleaning products and plant decors as hexanal and heptanal.[18]

Studies regarding organic acids and formaldehyde in museum environments have been done for decades.[14,19,20] They were usually related to quantification in the environment[8,10,12,15,21,22] without evaluating their interaction with artworks. A significant part of interaction studies deals with metals.[23-26] The work described in this article collaborates with another smaller portion of the literature, where studies use paints (real or simulations) or powdered pigments in tests.[2,27,28] Regarding hexanal and 2-butanone oxime, no studies analyzed pigments and paints degradation after exposure to such VOCs. Among countless artistic objects that may undergo interference caused by VOCs, paintings stand out because of their stability depending on the physical-chemical characteristics of each of their components, wherein the modification of these characteristics is referred to as degradation. Color change is one of the easiest deterioration characteristics to detect, as it compromises artwork. Common phenomena are fading, whitening, darkening, yellowing and manifestation of spots.[29-38] Yet, another common form of degradation is the formation of metallic carboxylate, once up to 70% of oil paintings in and around museums contain these subproducts.[39] From a preservation standpoint, the formation of these structures is highly prejudicial due to amounting into deposits which are tough to remove, insoluble and completely adhered to the painting.[40] In most cases, the presence of metallic soap makes the painting fragile and damages its structural integrity, which can be detected on account of protrusions, efflorescence, spots, darkening, dimming, loss of opacity or paint, sandy textures, and transparency.[31,39,41-44] Acknowledging how vital research regarding VOC within museum atmospheres is, it is clear that interactions between paint and pigments and these compounds, even the more common ones such as acetic acid and formic acid, are not widely understood.[24,45] Henceforth, there is a need for research surrounding interactions between several VOCs, inorganic pigments and binders used in paintings, evaluating the chromatic parameter shift and formation of metallic carboxylate, the first being caused by the organic portion of VOCs, the latter by the metallic portion within pigments. Studies regarding the effects of variations in the museum atmosphere have already been done. However, in order for these predictions to be made before any damage occurs, such studies are carried out in accelerated degradation situations to produce faster results and interfere in conservation processes before irreversible damage occurs.[2,32,33,37,46-49]

Experimental

Preparation of painting models

Paintings were prepared by employing a mixture of synthetic pigments of yellow cadmium (CdS, Manuel Riesgo S.A, Madri, Spain), chromium oxide (Cr_2O_3, Manuel Riesgo S.A, Madri, Spain) or ultramarine blue ($Na_8Al_6Si_6O_{24}S_2$, Manuel Riesgo S.A, Madri, Spain) and linseed oil (Titan, Barcelona, Spain) in the pigment/binder mass proportion of 1:0.25. Painting was carried out with a paintbrush on the surface of a cotton canvas. This support was cut into rectangles, with dimensions of 10 cm high and 4 cm wide (Figure 1), which were then fixed to a wooden base of the same size to maintain its shape. Some models were painted with a lead white primer ($2PbCO_3 \cdot Pb(OH)_2$, Sigma-Aldrich, St. Louis, USA) or gypsum ($CaSO_4 \cdot 2H_2O$, Sigma-Aldrich, St. Louis, USA) backdrop as a form of preparatory step used to flatten painting surfaces.[50] The types of models are: (*i*) only the paint pigment; (*ii*) lead white primer + pigment; (*iii*) gypsum primer + pigment.

Therefore, 3 different models were employed for each pigment type (with a total of 3 pigments) and exposed to 5 types of atmospheres (4 contaminated and 1 control), reaching a total of 45 samples, which were then put through Fourier transform infrared attenuated total reflection (FTIR-ATR) and colorimetry analysis. The drying time for primers and pigments was approximately 15 days for linseed oil paintings. Figure 1 exemplifies the preparation of models for malachite pigment.
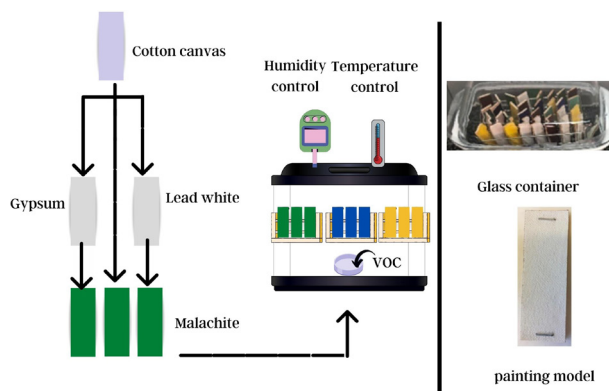

Figure 1. Making off and display of the painting models.

In order to confirm the yellowing process within some models, the experiment was then re-run with ultramarine blue and a water-based animal glue binder as

a replacement for linseed oil with the mass proportion of 1:2:4 (pigment:adhesive:water), repeating combinations (*ii*) and (*iii*), for a total of 10 samples.

Accelerated aging and analysis

After the paintings dried, they were exposed to VOC in an airtight glass container and positioned vertically with the help of a support structure of stainless steel (Figure 1). VOC saturated atmospheres were created by adding a small container with 98% glacial acetic acid (standard, Sigma-Aldrich, St. Louis, USA), 37% m/v formaldehyde, hexanal or 2-butanone oxime (standard, Sigma-Aldrich, St. Louis, USA). A control group was also produced. The environmental temperature was set to 25 °C, and relative humidity was between 50-60% (experiments were conducted in Madrid, Spain).

Color measurements were done with reflectance measurement equipment placed directly on model surfaces after 0, 7, 21 and 42 days of exposure. These times were considered adequate for a minimum number of color analyses to be carried out periodically, so the trend of changes could be presented. UV-Vis (Lambda 650, PerkinElmer, Shelton, USA) spectrometer was used within the range of 295 to 835 nm, with 5 nm intervals. According to the International Commission on Illumination (CIE, Commission Internationale de l'éclairage), this method allows for a quantitative approach, defined by luminosity parameter (L*) and coordinates that define color directions a* and b*. The CIE 1976 (L*, a*, b*) color system, CIELAB for short, presents an L* parameter which ranges from 0 (black) to 100 (white), and the coordinates indicate tonal shifts towards red (+a*), green (−a*), yellow (+b*) or blue (−b*). Color difference is calculated by subtracting the L*, a* and b* results of a control sample from a treated sample, thus obtaining the ΔL*, Δa* and Δb* variants. This information may be presented in a single numeric value (ΔE*, equation 1), indicating effective amounts of color shifts.[51] When ΔE* is higher than 5, color shifts are significant, and observers can visualize two distinct colors.[51,52]

$$\Delta E^* = \left(\left(\Delta L^* \right)^2 + \left(\Delta a^* \right)^2 + \left(\Delta b^* \right)^2 \right)^{\frac{1}{2}} \qquad (1)$$

Color discussion was based on more relevant colorimetric shifts, these being when samples simultaneously presented the following conditions: (*i*) ΔE* value above the tolerance limit of 5;[51,52] (*ii*) ΔE* value of the treated sample at most 1.5 times higher than the ΔE* value of the control sample.

Data regarding the infrared spectrum was obtained after 42 days of exposure via a spectrometer Fourier transformed infrared (FTIR) (Nicolet 5700, Thermo, Madison, USA) with a resolution of 1.93 cm⁻¹, spectral ranging from 4000 to 400 cm⁻¹, 124 scans and equipped with an attenuated total reflection (ATR) accessory, onto which the paintings were pressed directly over the ZnSe crystal. Superficial modifications to the paintings' surfaces were shown in the spectrum with presence or lack of characteristic bands connected to specific chemical bonds or functional groups.

In order to comprehend how the formation of metallic carboxylate affected painting topography, scanning electron microscopy (SEM) analysis was carried out (JEOL JSM 6400 Scanning Microscope, 20.00 KV, Work Distance (WD): 15 mm, Tokyo, Japan) with a secondary electron detector; thus, providing high-resolution images of sample surfaces. For the analysis, ultramarine blue models with lead white primer were selected, onto which there was carboxylate formation in the presence of acetic acid, formaldehyde and hexanal VOCs, whilst significant color variation was also observed.

Results and Discussion

Colorimetric measures

Ultramarine blue pigment showed significant color shifts in samples exposed to 2-butanone oxime, acetic acid, hexanal and formaldehyde (Figure 2). Color variation occurred with increased b* parameters (direction towards yellow) and decreased a* parameters (direction towards green), making the Pearson correlation coefficient (r) a reasonable estimate of the tendency (Δa* *versus* Δb*; r = −0.977). Total color variation (ΔE) occurred primarily due to these two simultaneous factors (ΔE *versus* Δa*; r = −0.987 and ΔE *versus* Δb*; r = 0.997).

Yellowing mainly affects blue and white pigments, giving the first a greenish hue since green is a secondary color obtained by mixing the blue and yellow primary colors.[53,54] The same color changing process from ultramarine blue to green was observed in real paintings and correlated to the yellowing of lipid binders such as linseed oil or egg yolk.[28,53] Verily, it is recommended that when preparing ultramarine paint, linseed oil be preferably replaced by binders that tend to undergo less yellowing, such as poppy or nut oil. Another recommendation is the replacement of lipid binders with water-based ones, such as Arabic gum and animal glue.[54]

In the ultramarine experiment (Figure 3), by substituting linseed oil with animal glue, no significant color variation was observed (ΔE < 5), except for the sample prepared with ultramarine, lead white primer and exposed to acetic acid (ΔE = 32). Hence, the color changing process in the experimental conditions with

Day 0 – Day 42	Day 0 – Day 42	Day 0 – Day 42	Day 0 – Day 42	Day 0 – Day 42
Control	2-Butanone Oxime	Acetic Acid	Hexanal	Formaldehyde
Ultramarine (monolayer)				
ΔE = 6	ΔE = 24	---	---	---
Gypsum primer + ultramarine layer				
ΔE = 11	ΔE = 37	ΔE = 28	---	---
Lead white primer + ultramarine layer				
ΔE = 7	ΔE = 28	ΔE = 40	ΔE = 23	ΔE = 24

Figure 2. Color simulation for both control and exposed samples, and ΔE values for ultramarine samples.

linseed oil was directly linked to its subsequent yellowing caused by VOC (Figure 2). For the exception presented in the conditions in which animal glue was used (Figure 3), formation of lead acetate may contribute to sample yellowing. It is noticeable that for samples prepared with ultramarine and linseed oil (Figure 2), this same composition (ultramarine + lead white primer + acetic acid exposure) presented the highest total color variation (ΔE = 40). This elevated color variation is explained due to the synergetic effect regarding both lipid binder yellowing and carboxylate formation. It is known that formed lead acetate, when impure, may present a brownish hue, which would justify sample yellowing. Furthermore, some paints which use lead acetate as a drying agent have shown a yellower hue, confirming these results.[55]

Significant color shifts also occurred for cadmium yellow when exposed to 2-butanone-oxime (Figure 4). A slight decrease in luminosity (L*) was observed in exposed samples.

For chromium oxide, all color alteration was both inferior to the limit for differentiating two colors (ΔE > 5) and for clear color distinction (3.5 < ΔE < 5).[52]

Yellowing of compounds such as linseed oil and natural resin favored by VOCs has already been previously mentioned in the literature. It has been shown to strongly affect final colors of ultramarine paintings.[56,57] This is due to these pigments' high transparency when mixed with linseed oil, given that both their refractive indexes are similar. Accordingly, the painting acquired greenish hues when the binder became yellow. The same did not occur
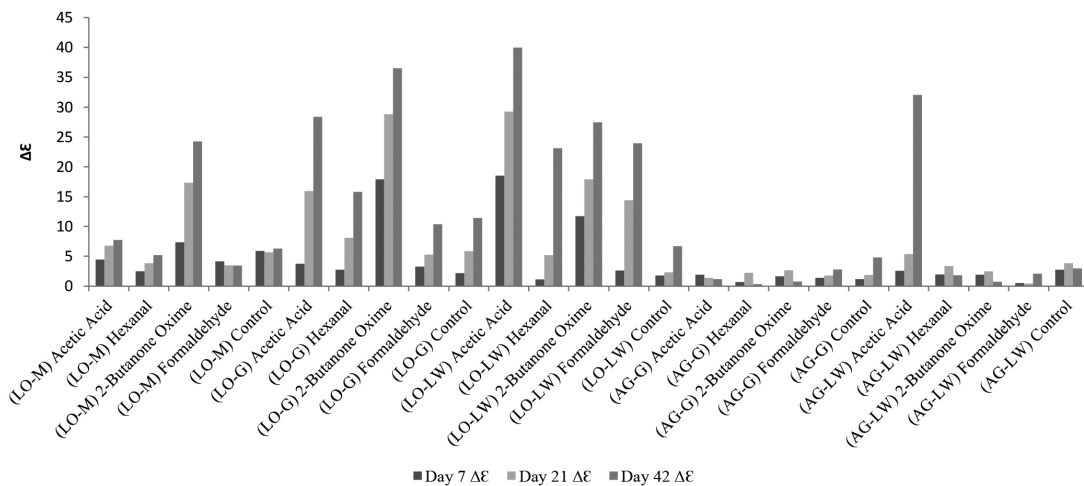

Figure 3. ΔE values for ultramarine samples prepared with linseed oil (LO) or animal glue (AG) exposed to VOC. Preparation conditions used: pigment in monolayer (M) or with lead white (LW) or gypsum (G) primer.
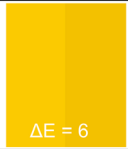
Figure 4. Color simulation for both control and exposed samples and ΔE values for cadmium yellow samples.

for chromium oxide and cadmium yellow, which both have a relatively high disparity concerning the linseed oil refractive index, compared to ultramarine blue, conferring these paints higher opacity. Cadmium yellow, in addition

to its opacity, is naturally yellow, which also decreases yellowing impacts.[54,58]

FTIR-ATR analysis

Ultramarine blue, cadmium yellow, and chromium oxide pigments combined with gypsum did not show interactions with selected VOCs. However, when lead white primer was used, lead carboxylate formed in addition to decreased bands in 1392 and 679 cm^{-1} regarding the CO_3^{2-} group stretches (Figures 5-7). Lead acetate, formate and hexanoate were formed in the ultramarine blue models (Figure 5), and lead acetate and hexanoate were formed in the cadmium yellow models (Figure 6).

Only lead acetate was formed for the chromium oxide pigment (Figure 7). This indicates that chromium oxide might have acted as a more effective protective layer for lead white primer when compared to ultramarine blue or cadmium yellow. This result is likely related to the fact that this pigment has catalytic activities in the degradation processes of other compounds, which may have interfered with VOCs; however, further research is required.[59,60] Chromium oxides are generally considered highly stable, and there are not many works concerning their degradation, only studies indicating the pigment's presence in paintings.[61-65]

Figure 5. FTIR-ATR spectra for models made with lead white prime and an ultramarine layer. Black + highlights carboxylate absorption; black * highlights decreased lead white absorption, and black X highlights increased ultramarine absorption (658 and 687 cm^{-1}).

Figure 6. FTIR-ATR spectra for models with lead white primer and a cadmium yellow layer. Black + highlights carboxylate absorption; black * highlights decreased white lead absorption, and black X highlights cotton absorption.
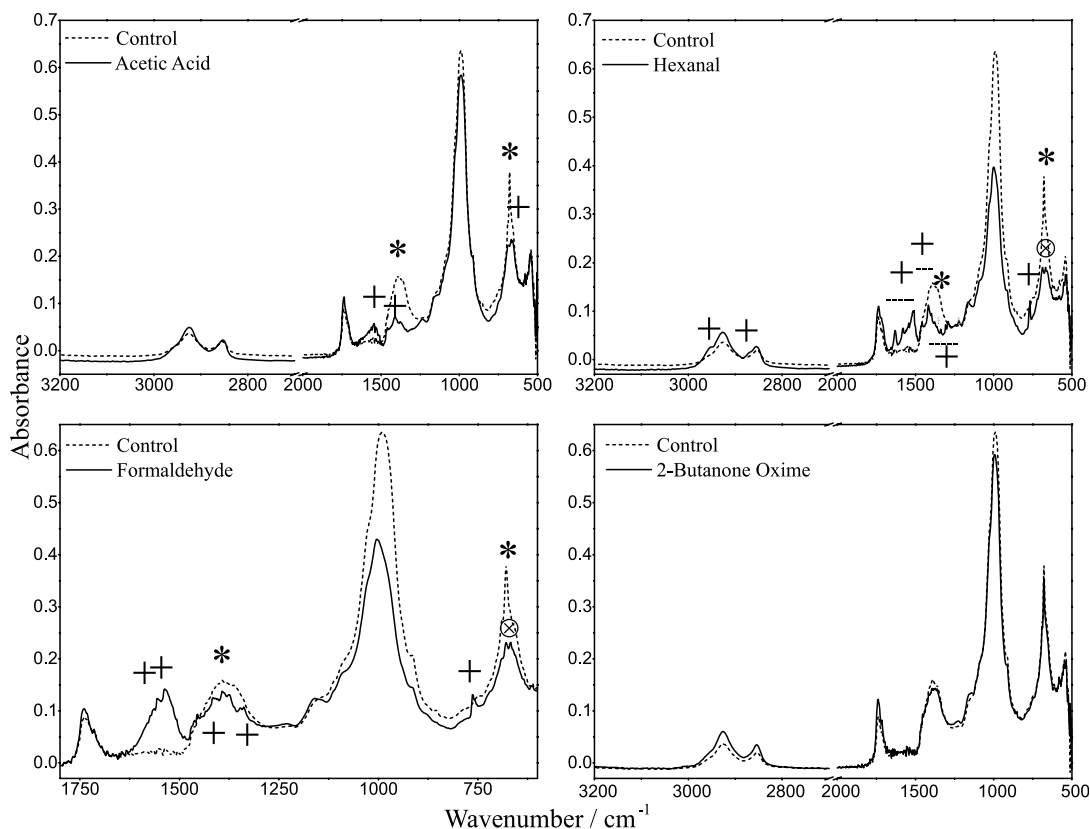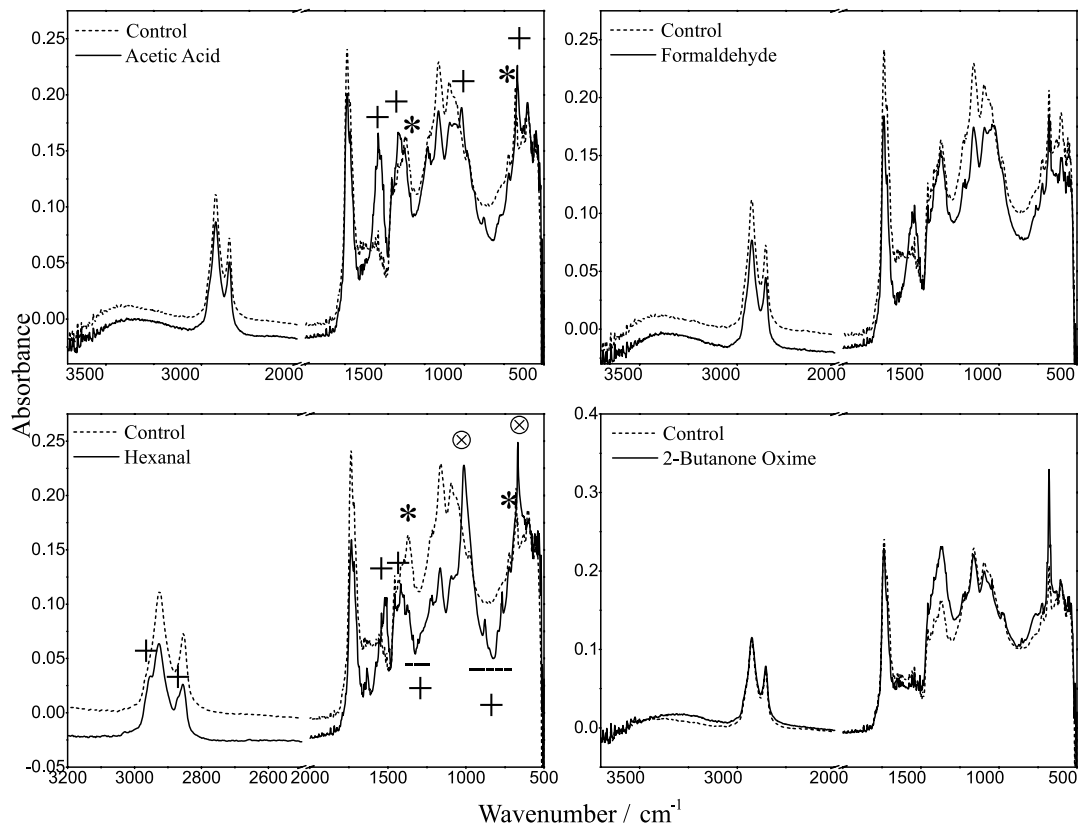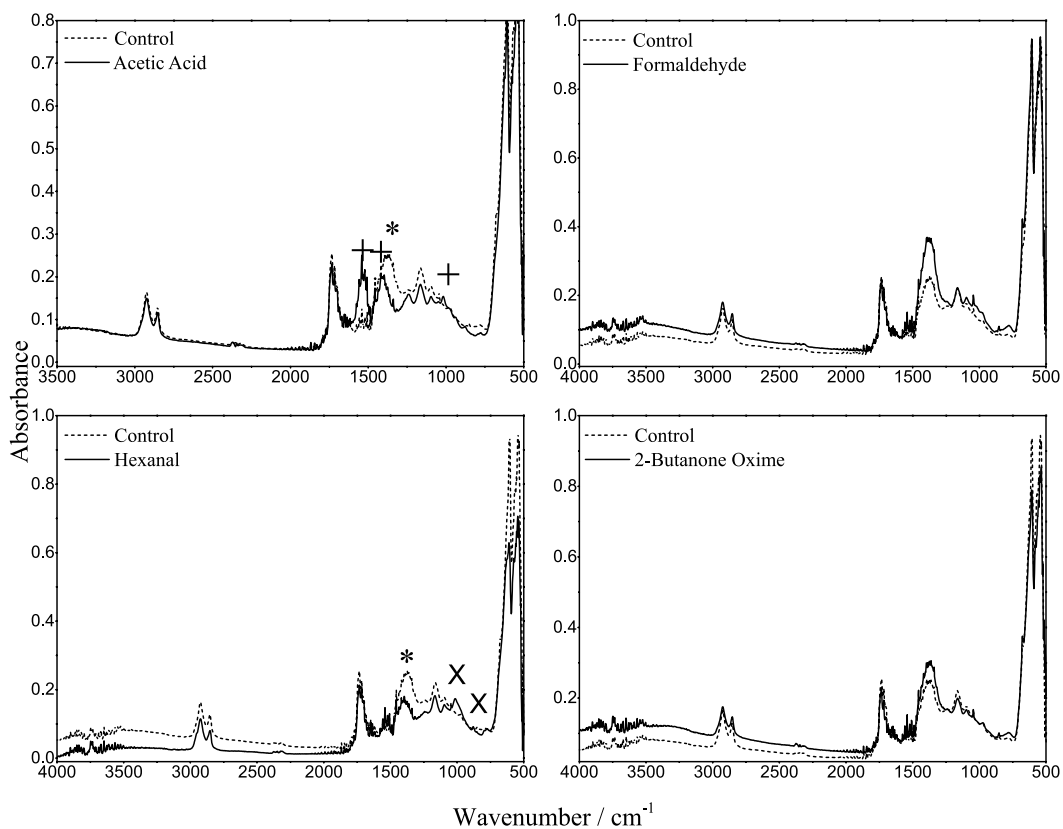

Figure 7. FTIR-ATR spectra for models with lead white primer and a chromium oxide layer. Black + highlights carboxylate absorption; black * highlights decreased lead white absorption, and black X highlights cotton absorption.

Other spectra not discussed (pure pigments and pigments added to gypsum primer) are available in Figures S1-S6 of the Supplementary Information (SI) section.

Tables 1-3 present bands referring to each formed carboxylate.

Table 1 describes bands referring to lead acetate formed in the three pigment models. Bands that occur at approximately 1405 and 1540 cm^{-1} are due to symmetrical and asymmetrical stretches, respectively, of the C−O vibration, both of the acetate ion (COO$^-$). The band at 660 cm^{-1} refers to folding to the same functional group.[66,67]

Table 2 describes the lead hexanoate bands formed in the ultramarine blue and cadmium yellow models. Absorptions that confirm the formation of this lead carboxylate are the bands at 1542-1512 and 1400-1420 cm^{-1}, referring to asymmetric and symmetric stretching of the carboxyl, respectively. Bands between 1150 and 1350 cm^{-1} refer to the wagging and twisting vibrations of the hydrocarbon chain. The band at 725 cm^{-1} is also due to the hydrocarbon chain (rocking folding for hydrocarbons with more than 4 methylene groups).

Table 3 describes lead formate bands formed only in models with ultramarine blue. Bands at 1338/1347 cm^{-1} (mode 2) and 1537/1555 cm^{-1} (mode 4) are related to the symmetric and asymmetric OCO$^-$ stretching from lead formate, respectively. This last band suffered a shift to a lower frequency, probably due to the interaction between the carboxyl and the pigment surface. In general, spectra of metallic carboxylates can vary mainly due to shifts in the frequencies of modes 2 and 4 of the carboxyl vibrations (as seen for mode 4) and the possibility of band division due to the type of crystalline structure formed. Regarding the second factor, modes 4 and 6 occasionally appear as doublets, whereas modes 2, 3 and 5 may appear more frequently in divided bands.[73] Bands at 762 cm^{-1} (mode 3) and 1376/1392 cm^{-1} (mode 5) refer to the OCO$^-$ folding for the same compound.

Frequently cited carboxylate in literature, also known as metallic soaps, are formed primarily from reactions between metals, such as lead, calcium and zinc, contained in pigments and free fatty acids in binders, lipids such as linseed oil and egg yolk.[56,75-78] In the experiment mentioned above, however, carboxylic acids did not come from linseed oil but from VOCs instead, which have just recently begun being discussed in the literature.

Table 1. Values concerning formed lead acetate bands for each pigment compared with the standard compound

Carboxylate in ultramarine sample / cm^{-1}	Carboxylate in cadmium yellow sample / cm^{-1}	Carboxylate in chromium oxide sample / cm^{-1}	Lead acetate / cm^{-1}	Assignment
1544	1540	1536	1540[68]	$\nu_{as}COO^-$
1412	1415	1410	1405[68]	ν_sCOO^-
–	–	–	1335[68]	$\delta_{as}CH_3$
Possibly overlaid to the wide band centered at 980 cm^{-1} of ultramarine blue	1018 –	1015 –	1015[67] 932[68]	$\nu C-C$ $\nu C-C$
668	667	possibly overlaid to the wide band centered at 610 cm^{-1} of chromium oxide	660[66,68]	δOCO^-

ν: stretching; *δ*: folding; s: symmetric; as: asymmetric.

Table 2. Values concerning formed lead hexanoate bands for each pigment compared with the standard compound

Carboxylate in ultramarine sample / cm^{-1}	Carboxylate in cadmium yellow sample / cm^{-1}	Lead hexanoate / cm^{-1}	Assignment
2951	2952	2955/2920[69]	$\nu_aCH_3\,\nu_aCH_{2\,resp}$
2870	2870	2870/2850[69]	$\nu_sCH_3\,\nu_sCH_{2\,resp}$
1541-1510	1512	1542-1512[69]	ν_aCOO^-
–	–	1472/1465/1460[69]	δCH_2 and CH_3
–	–	1435[69]	δCH_2
1399-1416	1418	1400-1420[69,70]	ν_sCOO^-
–	–	1380[71]	δ_sCH_3
1164-1337	1350-1300	1150-1350[69-72]	δCH_2 (wagging, twisting)
777/768	768-878	700-1100[69]	δCH_2 (rocking)

ν: stretching; *δ*: folding; s: symmetric; as: asymmetric; resp: respectively.

Table 3. Values concerning formed lead formate bands for each pigment compared with the standard compound

Carboxylate in ultramarine sample / cm^{-1}	Lead formate[73] / cm^{-1}	Lead formate[74] / cm^{-1}	Assignment
–	2833	–	vCH (mode 1)
1537/1555	1577	1530/1580	v_{as}OCO$^-$ (mode 4)
1376/1392	1372/1389	1390	δ_{as}OCO$^-$ (mode 5)
1338/1347	1333/1348	1350	v_sOCO$^-$ (mode 2)
–	1066/1075	–	δOCO$^-$ out of the field (mode 6)
762	758/763	760	δ_sOCO$^-$ (mode 3)

v: stretching; δ: folding; s: symmetric; as: asymmetric.

SEM for ultramarine blue-control micrographs

The model prepared exclusively with ultramarine blue (Figure 8a) presented a grainy, round and relatively regularly sized morphology and some round crevasses characteristic of ultramarine blue.[79,80] In the sample with lead white primer (Figure 8b), the grainy and round morphology of ultramarine blue is mixed with the appearance of flat, tabular and hexagonally shaped particles characteristic of lead white pigment.[81]

VOC exposure

Only samples with metallic carboxylate formation that is, samples in which lead white was utilized as a primer, presented surface changes compared with the control. When exposed to acetic acid, the paint's granular aspect shifted towards a smoother, homogenous surface with a few cracks (Figure 8c). X-ray energy dispersion spectroscopy analysis results (EDX, Figure S7 in the SI section) show that lead is found in the micrograph dark region and not in lighter regions (cracked region). It is likely that in the first region (highlighted in red), lead acetate was deposited, leading to apparent changes. In the second region (highlighted in blue), cracked areas are shown, where only elements pertaining to ultramarine blue were found (Al, Si, Na and S). Thus, cracked areas may be interpreted as regions with no lead acetate deposits, maintaining the original painting. Results for hexanal exposure were similar to those obtained for acetic acid exposure, although smaller in scale (Figure 8d). In some regions, a smooth layer was formed over the paint's granular surface, probably due to formation of lead hexanoate. EDX analysis results (Figure S8 in SI section) show that the element lead is found in the dark smooth region of the micrograph (highlighted in red, lead hexanoate) and was not found in the light grainy region (highlighted in blue, ultramarine).

These micrographs show that the ultramarine blue pigment did not suffer any direct effects caused by exposure, which did affect the lead white primer. Henceforth, the mobile capacity of metallic soaps and their tendency to migrate from internal layers towards painting surfaces ought to be discussed.[76] Formation of lead soap from lead white used as a primer layer may significantly modify the appearance of several paintings; therefore, this effect must be closely observed and discussed. Paints are a semi-permeable system that may be influenced by physical factors such as micro-fissures, nanopores, climate variation[77,82] and atmospheric pollution. The best documented conditions contributing to formation of metallic soaps are humidity, luminosity and temperature; however, understanding how each of these factors acts is yet to be optimal. What is already clear is that this process is spontaneous, irreversible and generally influenced by the concentration of metallic ions and free carboxylic acids, in addition to forming a low solubility product.[41,43,77,79]

Degradation of specific painting components may promote several visual alterations, such as darkening, color, tone and contrast shifts, and loss of detail, which negatively impact its aesthetics and preservation.[76,83] Regarding carboxylate formation, it is very likely that lead white goes through initial dissolution, leading to carboxylates being found in deposits along the darkest regions, with higher organic content from VOCs. Lead soap micrographs, commonly found in literature, are formed in areas containing lead particles with affected or disintegrated edges and lead-rich undefined areas. Thus, the total or partial lead white particle dissolution process originates in saponified regions.[84]

Conclusions

Previous experiments allowed for further comprehension of the interaction between VOCs, inorganic pigments and binders used in paintings. Concerning chromatic parameters, yellowing which affects linseed oil caused by VOC interactions, modified the ultramarine blue color with a greenish tint. A lowered luminosity was the most
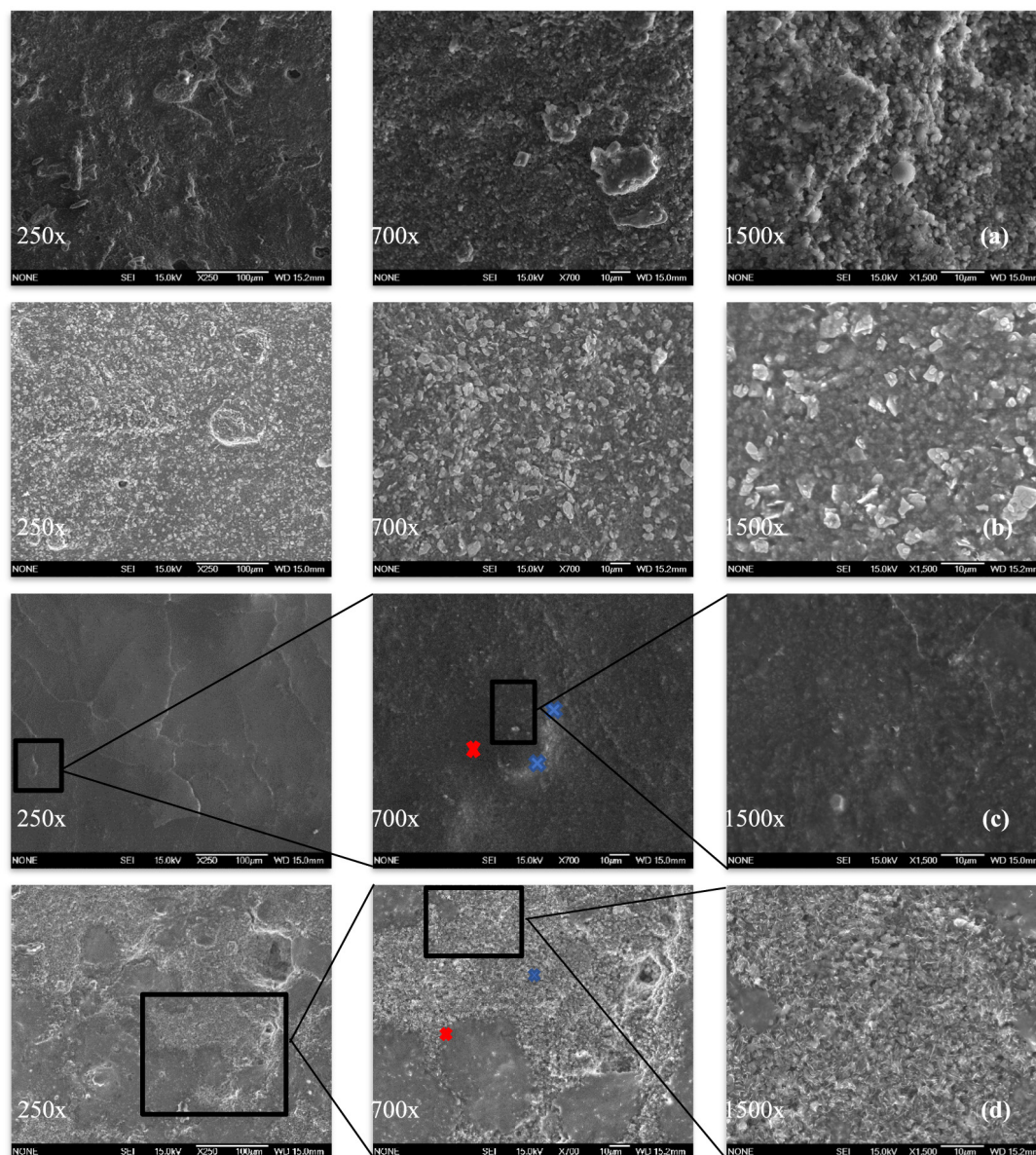
Figure 8. Control micrographs: (a) ultramarine; (b) ultramarine + lead white primer. Exposed sample micrographs: (c) lead acetate; (d) lead hexanoate. Enlargements are highlighted in black.

distinguishable change for the models with cadmium yellow or chromium oxide. For chromium oxide, there were no noticeable color changes higher than the established limit for differentiating between two colors ($\Delta E > 5$). Regarding the formation of metallic carboxylate (when lead white was used as a primer) several lead carboxylates were formed, such as lead acetate, formate and hexanoate for the models with cadmium yellow and lead acetate for the models with chromium oxide. The topography of ultramarine blue models containing carboxylates showed that the painting's granular aspect was replaced by a smooth and homogenous appearance, being this the place where saponification occurred due to the dissolution of lead white particles.

Supplementary Information

Supplementary information (Figures S1-S8) is available free of charge at http://jbcs.sbq.org.br as PDF file.

Acknowledgments

References

1. Marengo, E.; Liparota, M. C.; Robotti, E.; Bobba, M.; Gennaro, M. C.; *Anal. Bioanal. Chem.* **2005**, *381*, 884. [Crossref]

2. De Laet, N.; Lycke, S.; Van Pevenage, J.; Moens, L.; Vandenabeele, P.; *Eur. J. Mineral.* **2014**, *25*, 855. [Crossref]

3. Schieweck, A.; Salthammer, T.; Watts, S. F. In *Organic Indoor Air Pollutants*; Wiley-VCH Verlag GmbH & Co. KGaA: Weinheim, Germany, 2009.

4. PennState College of Earth and Mineral Science, *Changes in Atmospheric Composition*, https://www.e-education.psu.edu/meteo300/node/606, accessed in March 2023.

5. Turiel, I.; Hollowell, C. D.; Miksch, R. R.; *Atmos. Environ.* 1983, *17*, 51. [Crossref]

6. United State Environmental Protection Agency, *Indoor Air Quality (IAQ)*, http://www.epa.gov/iaq/ia-intro.html, accessed in March 2023.

7. Zhang, Y.; *Indoor Air Quality Engineering*, vol. 1, 1st ed.; CRC Press: Boca Raton, United States, 2004.

8. Schieweck, A.; Lohrengel, B.; Siwinski, N.; Genning, C.; Salthammer, T.; *Atmos. Environ.* **2005**, *39*, 6098. [Crossref]

9. Sanchez, B. C.; Vilanova, O.; Canela, M. C.; Espinosa, T. G.; *Boletín del Museo Arqueológico Nacional*, vol. 38, 1st ed.; Ministerio de cultura y deporte: Madrid, Espanha, 2015.

10. Sánchez, B.; Souza, M. O.; Vilanova, O.; Canela, M. C.; *Build. Environ.* **2020**, *174*, 106780. [Crossref]

11. Campagnolo, D.; Saraga, D. E.; Cattaneo, A.; Spinazzè, A.; Mandin, C.; Mabilia, R.; Perreca, E.; Sakellaris, I.; Canha, N.; Mihucz, V. G.; Szigeti, T.; Ventura, G.; Madureira, J.; de Oliveira Fernandes, E.; de Kluizenaar, Y.; Cornelissen, E.; Hänninen, O.; Carrer, P.; Wolkoff, P.; Cavallo, D. M.; Bartzis, J. G.; *Build. Environ.* **2017**, *115*, 18. [Crossref]

12. Fenech, A.; Strlič, M.; Kralj Cigić, I.; Levart, A.; Gibson, L. T.; de Bruin, G.; Ntanos, K.; Kolar, J.; Cassar, M.; *Atmos. Environ.* **2010**, *44*, 2067. [Crossref]

13. Oikawa, T.; Matsui, T.; Matsuda, Y.; Takayama, T.; Niinuma, H.; Nishida, Y.; Hoshi, K.; Yatagai, M.; *J. Wood Sci.* **2005**, *51*, 363. [Crossref]

14. Grzywacz, M. C.; *Monitoring for Gaseous Pollutants in Museum Environments*; Getty Publications: Los Angeles, United States, 2006.

15. Godoi, R. H. M.; Carneiro, B. H. B.; Paralovo, S. L.; Campos, V. P.; Tavares, T. M.; Evangelista, H.; Van Grieken, R.; Godoi, A. F. L.; *Sci. Total Environ.* **2013**, *452-453*, 314. [Crossref]

16. Vila Nova, O. M. V.: *Identificación, Cuantificación Evaluación y Tratamiento de VOCS en Ambiente Interior*; PhD Thesis, Universidad Autonoma de Madrid, Madrid, Espanha, 2018. [Crossref]

17. Schieweck, A.; Salthammer, T.; *J. Cult. Heritage* **2011**, *12*, 205. [Crossref]

18. Souza, M. O.; Vieira, H. G.; Sánchez, B.; Canela, M. C.; *Quim. Nova* **2021**, *44*, 830. [Crossref]

19. Baer, N.; *Mus. Manage. Curatorship* **1985**, *4*, 9.

20. Hatchfield, P.; Carpenter, J. M.; *J. Mater. Sci.* **1986**, *5*,183.

21. Cincinelli, A.; Martellini, T.; Amore, A.; Dei, L.; Marrazza, G.; Carretti, E.; Belosi, F.; Ravegnani, F.; Leva, P.; *Sci. Total Environ.* **2016**, *572*, 333. [Crossref]

22. Martellini, T.; Berlangieri, C.; Dei, L.; Carretti, E.; Santini, S.; Barone, A.; Cincinelli, A.; *Indoor Air* **2020**, *30*, 900. [Crossref]

23. de Faria, D. L. A.; Puglieri, T. S.; Souza, L. A. C.; *J. Braz. Chem. Soc.* **2013**, *24*, 1345. [Crossref]

24. Nodari, L.; Tresin, L.; Benedetti, A.; Tufano, M. K.; Tomasin, P.; *J. Cult. Heritage* **2019**, *35*, 288. [Crossref]

25. Raychaudhuri, M. R.; Brimblecombe, P.; *Stud. Conserv.* **2013**, *45*, 226. [Crossref]

26. Strachotová, K. C.; Kouřil, M.; *Koroze Ochr. Mater.* **2018**, *62*, 87. [Crossref]

27. La Nasa, J.; Degano, I.; Modugno, F.; Colombini, M. P.; *Polym. Degrad. Stab.* **2014**, *105*, 257. [Crossref]

28. Herrera, A.; Ballabio, D.; Navas, N.; Todeschini, R.; Cardell, C.; *Chemom. Intell. Lab. Syst.* **2017**, *167*, 113. [Crossref]

29. Gunn, M.; Chottard, G.; Rivière, E.; Girerd, J. J.; Chottard, J.-C.; *Stud. Conserv.* **2002**, *47*, 12. [Crossref]

30. Ioakimoglou, E.; Boyatzis, S.; Argitis, P.; Fostiridou, A.; Papapanagiotou, K.; Yannovits, N.; *Chem. Mater.* **1999**, *11*, 2013. [Crossref]

31. Mazzeo, R.; Prati, S.; Quaranta, M.; Joseph, E.; Kendix, E.; Galeotti, M.; *Anal. Bioanal. Chem.* **2008**, *392*, 65. [Crossref]

32. Harrison, J.; Lee, J.; Ormsby, B.; Payne, D. J.; *Heritage Sci.* **2021**, *9*, 107. [Crossref]

33. Maguregui, M.; Castro, K.; Morillas, H.; Trebolazabala, J.; Knuutinen, U.; Wiesinger, R.; Schreiner, M.; Madariaga, J. M.; *Anal. Methods* **2014**, *6*, 372. [Crossref]

34. Mass, J.; Sedlmair, J.; Patterson, C. S.; Carson, D.; Buckley, B.; Hirschmugl, C.; *Analyst* **2013**, *138*, 6032. [Crossref]

35. Richardson, E.; Woolley, E.; Yurchenko, A.; Thickett, D.; *J. Illum. Eng. Soc.* **2020**, *16*, 67. [Crossref]

36. Sarmiento, A.; Maguregui, M.; Martinez-Arkarazo, I.; Angulo, M.; Castro, K.; Olazábal, M. A.; Fernández, L. A.; Rodríguez-Laso, M. D.; Mujika, A. M.; Gómez, J.; Madariaga, J. M.; *J. Raman Spectrosc.* **2008**, *39*, 1042. [Crossref]

37. Schnetz, K.; Gambardella, A. A.; van Elsas, R.; Rosier, J.; Steenwinkel, E. E.; Wallert, A.; Iedema, P. D.; Keune, K.; *J. Cult. Heritage* **2020**, *45*, 25. [Crossref]

38. Zoppi, A.; Lofrumento, C.; Mendes, N. F. C.; Castellucci, E. M.; *Anal. Bioanal. Chem.* **2010**, *397*, 841. [Crossref]

39. Izzo, F. C.; Kratter, M.; Nevin, A.; Zendri, E.; *ChemistryOpen* **2021**, *10*, 904. [Crossref]

40. van Loon, A.: *Color Changes and Chemical Reactivity in Seventeenth-Century Oil Paintings*; PhD Thesis, University of Amsterdam, Amsterdam, Netherlands, 2008. [Link] accessed in May 2023

41. Garrappa, S.; Kočí, E.; Švarcová, S.; Bezdička, P.; Hradil, D.; *Microchem. J.* **2020**, *156*, 104842. [Crossref]

42. van Loon, A.; Hoppe, R.; Keune, K.; Hermans, J. J.; Diependaal, H.; Bisschoff, M.; Thoury, M.; van der Snickt, G.; In *Metal*

Soaps in Art; Casadio, F.; Keune, K.; Noble, P.; Van Loon, A.; Hendriks, E.; Centeno, S. A.; Osmond, G., eds; Springer: Cham, 2019, p. 359. [Crossref]

43. Platania, E.; Streeton, N. L. W.; Lluveras-Tenorio, A.; Vila, A.; Buti, D.; Caruso, F.; Kutzke, H.; Karlsson, A.; Colombini, M. P.; Uggerud, E.; *Microchem. J.* **2020**, *156*, 104811. [Crossref]

44. Possenti, E.; Colombo, C.; Realini, M.; Song, C. L.; Kazarian, S. G.; *Anal. Bioanal. Chem.* **2021**, *413*, 455. [Crossref]

45. Duce, C.; Bramanti, E.; Ghezzi, L.; Bernazzani, L.; Bonaduce, I.; Colombini, M. P.; Spepi, A.; Biagi, S.; Tine, M. R.; *Dalton Trans.* **2013**, *42*, 5975. [Crossref]

46. Cato, E.; Borca, C.; Huthwelker, T.; Ferreira, E. S. B.; *Microchem. J.* **2016**, *126*, 18. [Crossref]

47. Melchiorre Di Crescenzo, M.; Zendri, E.; Sánchez-Pons, M.; Fuster-López, L.; Yusá-Marco, D. J.; *Polym. Degrad. Stab.* **2014**, *107*, 285. [Crossref]

48. Maguregui, M.; Knuutinen, U.; Castro, K.; Madariaga, J. M.; *J. Raman Spectrosc.* **2010**, *41*, 1400. [Crossref]

49. Barberio, M.; Skantzakis, E.; Sorieul, S.; Antici, P.; *Sci. Adv.* **2019**, *5*, 1. [Crossref]

50. Bracci, S.; Caruso, O.; Galeotti, M.; Iannaccone, R.; Magrini, D.; Picchi, D.; Pinna, D.; Porcinai, S.; *Spectrochim. Acta, Part A* **2015**, *145*, 511. [Crossref]

51. Minolta, K.; *Precise Color Communication: Color Control from Perception to Instrumentation*; Konica Minolta Sensing Inc.: Japan, 2007.

52. Mokrzycki, W.; Tatol, M.; *Mach. Graph. Vis.* **2011**, *20*, 383.

53. van Loon, A.; Speleers, L.; Ferreira, E.; Keune, K.; Boon, J.; *Stud. Conserv.* **2006**, *51*, 217. [Crossref]

54. Hommes, M. H. E.: *Discoloration in Renaissance and Baroque Oil Paintings. Instructions for Painters, Theoretical Concepts, and Scientific Data*; PhD Thesis, Universiteit van Amsterdam, Amsterdam, Netherlands, 2002. [Link] accessed in April 2023

55. Carlyle, L.; Binnie, N.; Kaminska, E.; Ruggles, A.; *The Yellowing/Bleaching of Oil Paintings and Oil Paint Samples, Including the Effect of Oil Processing, Driers and Mediums on the Colour of Lead White Paint*; ICOM-CC 13th Triennial Meeting Preprints: London, 2002. [Link] accessed in May 2023

56. Townsend, J.; *The Yellowing/Bleaching Behaviour of Oil Paint: Further investigations into Significant Colour Change in Response to Dark Storage Followed by Light Exposure*; ICOM-CC 16th Triennial Conference: Lisbon, 2011. [Link] accessed in May 2023

57. Dahlin, E.; *Improved Protection of Paintings During Exhibition, Storage and Transit*; Norwegian Institute for Air Research: Kjeller, Norway, 2010.

58. Tahk, C.; *J. Am. Inst. Conserv.* **1979**, *19*, 3. [Crossref]

59. Anandan, K.; Rajendran, V.; *Mater. Sci. Semicond. Process.* **2014**, *19*, 136. [Crossref]

60. Magalhães, F.; Pereira, M. C.; Botrel, S. E. C.; Fabris, J. D.; Macedo, W. A.; Mendonça, R.; Lago, R. M.; Oliveira, L. C. A.; *Appl. Catal., A* **2007**, *332*, 115. [Crossref]

61. Buscaglia, M. B.; Halac, E. B.; Reinoso, M.; Marte, F.; *J. Cult. Heritage* **2020**, *44*, 27. [Crossref]

62. Christiansen, M. B.; Baadsgaard, E.; Sanyova, J.; Simonsen, K. P.; *Heritage Sci.* **2017**, *5*, 39. [Crossref]

63. Chua, L.; Hoevel, C.; Smith, G. D.; *Heritage Sci.* **2016**, *4*, 25. [Crossref]

64. Fuster-López, L.; Izzo, F. C.; Andersen, C. K.; Murray, A.; Vila, A.; Picollo, M.; Stefani, L.; Jiménez, R.; Aguado-Guardiola, E.; *SN Appl. Sci.* **2020**, *2*, 2159. [Crossref]

65. Pozzi, F.; Arslanoglu, J.; Cesaratto, A.; Skopek, M.; *J. Cult. Heritage* **2019**, *35*, 209. [Crossref]

66. Ito, K.; Bernstein, H. J.; *Can. J. Chem.* **1956**, *34*, 170. [Crossref]

67. Max, J. J.; Chapados, C.; *J. Phys. Chem. A* **2004**, *108*, 3324. [Crossref]

68. Harrison, P. G.; Healy, M. A.; *Inorg. Chim. Acta* **1983**, *80*, 279. [Crossref]

69. Arenas, A. S.; Garcia, M. V.; Redondo, M. I.; Cheda, J. A. R.; Roux, M. V.; Turrion, C.; *Liq. Cryst.* **1995**, *18*, 431. [Crossref]

70. Refat, M. S.; El-Korashy, S. A.; Kumar, D. N.; Ahmed, A. S.; *Spectrochim. Acta, Part A* **2008**, *70*, 217. [Crossref]

71. Catalano, J.; Murphy, A.; Yao, Y.; Yap, G. P. A.; Zumbulyadis, N.; Centeno, S. A.; Dybowski, C.; *Dalton Trans.* **2015**, *44*, 2340. [Crossref]

72. Mesubi, M. A.; *J. Mol. Struct.* **1982**, *81*, 61. [Crossref]

73. Donaldson, J. D.; Knifton, J. F.; Ross, S. D.; *Spectrochim. Acta* **1964**, *20*, 847. [Crossref]

74. Puglieri, T. S.; Freitas, R. O.; Maia, F. C. B.; de Faria, D. L. A.; *Quim. Nova* **2019**, *42*, 1050. [Crossref]

75. Izzo, F. C.; Kratter, M.; Nevin, A.; Zendri, E.; *ChemistryOpen* **2021**, *10*, 904. [Crossref]

76. Molinari, S.; *CeROArt* **2014**, 1. [Crossref]

77. Romano, C.; Lam, T.; Newsome, G. A.; Taillon, J. A.; Little, N.; Tsang, J.-s.; *Stud. Conserv.* **2020**, *65*, 14. [Crossref]

78. Salvadó, N.; Butí, S.; Labrador, A.; Cinque, G.; Emerich, H.; Pradell, T.; *Anal. Bioanal. Chem.* **2011**, *399*, 3041. [Crossref]

79. Flores-Sasso, V.; Pérez, G.; Ruiz-Valero, L.; Martínez-Ramírez, S.; Guerrero, A.; Prieto-Vicioso, E.; *Materials* **2021**, *14*, 6866. [Crossref]

80. Plesters, J.; *Stud. Conserv.* **1966**, *11*, 62. [Crossref]

81. Gettens, R. J.; Kühn, H.; Chase, W. T.; Kuhn, H.; *Stud. Conserv.* **1967**, *12*, 125. [Crossref]

82. Zeng, Q. G.; Zhang, G. X.; Leung, C. W.; Zuo, J.; *Microchem. J.* **2010**, *96*, 330. [Crossref]

83. Noble, P.; van Loon, A.; Boon, J. J.; *Preparation for Painting: The artist's Choice and Its Consequences*; ICOM International Committee for Conservation, Working group "Paintings: Scientific study, conservation and restoration": London, 2008.

84. Keune, K.; Van Loon, A.; Boon, J. J.; *Microsc. Microanal.* **2011**, *17*, 696. [Crossref]